



Citation for published version:

Ngwompo, RF & Galindo, R 2017, 'Passivity analysis of linear physical systems with internal energy sources modelled by bond graphs', Proceedings of the Institution of Mechanical Engineers, Part I: Journal of Systems and Control Engineering, vol. 231, no. 1, pp. 14-28. <https://doi.org/10.1177/0959651816682144>

DOI:

[10.1177/0959651816682144](https://doi.org/10.1177/0959651816682144)

Publication date:

2017

Document Version

Peer reviewed version

[Link to publication](#)

Ngwompo, RF. Galindo, R., Passivity analysis of linear physical systems with internal energy sources modelled by bond graphs, Proceedings of the Institution of Mechanical Engineers, Part I: Journal of Systems and Control Engineering, Volume: 231 issue: 1, page(s): 14-28. Copyright © 2017 IMechE. Reprinted by permission of SAGE Publications.

University of Bath

General rights

Copyright and moral rights for the publications made accessible in the public portal are retained by the authors and/or other copyright owners and it is a condition of accessing publications that users recognise and abide by the legal requirements associated with these rights.

Take down policy

If you believe that this document breaches copyright please contact us providing details, and we will remove access to the work immediately and investigate your claim.

Passivity Analysis of Linear Physical Systems with Internal Energy Sources Modelled by Bond Graphs

Journal Title
XX(X):1-27
©The Author(s) 2016
Reprints and permission:
sagepub.co.uk/journalsPermissions.nav
DOI: 10.1177/ToBeAssigned
www.sagepub.com/

Roger F Ngwompo¹ and René Galindo²

Abstract

Integrated dynamic systems such as mechatronic or control systems generally contain passive elements and internal energy sources that are appropriately modulated to perform the desired dynamic actions. The overall passivity of such systems is a useful property that relates to the stability and the safety of the system, in the sense that the maximum net amount of energy that the system can impart to the environment is limited by its initial state. In this paper, conditions under which a physical system containing internal modulated sources is globally passive are investigated using bond graph modelling techniques. For the class of systems under consideration, bond graph models include power bonds and active (signals) bonds modulating embedded energy sources, so that the continuity of power (or energy conservation) in the junction structure is not satisfied. For the purpose of the analysis, a so-called bond graph *pseudo junction structure* is proposed as an alternative representation for Linear Time-Invariant (LTI) bond graph models with internal modulated sources. The pseudo junction structure highlights the existence of a multiport coupled resistive field involving the modulation gains of the internal sources and the parameters of dissipative elements, therefore implicitly realising the balance of internal energy generation and dissipation. Moreover, it can be regarded as consisting of an *inner* structure which satisfies the continuity of power, and an *outer* structure in which a power scaling is performed in relation with the dissipative field. The associated multiport coupled resistive field constitutive equations can then be used to determine the passivity property of the overall system. The paper focuses on systems interconnected in cascade (with no loading effect) or in closed-loop configurations which are common in control systems.

Keywords

Bond graph, passivity, junction structure, cascade interconnection, dissipative systems, conservative systems.

¹ Department of Mechanical Engineering, Faculty of Engineering and Design, University of Bath Bath, BA2 7AY, UK
Email: R.F.Ngwompo@bath.ac.uk

²Autonomous University of Nuevo Leon, Faculty of Electrical and Mechanical Engineering, Av. Universidad, San Nicolas de los Garza, Nuevo Leon, 66450, Mexico.

Corresponding author:

R. F. Ngwompo Department of Mechanical Engineering, Faculty of Engineering and Design, University of Bath Bath, BA2 7AY, UK
Email: R.F.Ngwompo@bath.ac.uk

Introduction

Passivity is an interesting and important property in the design of integrated systems, such as control systems or mechatronic devices in general. In short, a system is said to be passive (or dissipative) if it can only store, release or dissipate energy without the possibility of generating energy. The interest of passivity is that it ensures the overall system stability. Also, it somehow relates to the idea of safety for systems interacting with the environment or human operators as the amount of energy that can be imparted to the environment by such systems is limited compared to nonpassive systems [7]. An obvious example is that in the absence of external energy supply, the maximum amount of energy that can be extracted from a passive system is limited by the initial energy stored whereas a nonpassive system may generate more energy that could be unsafe for the system it is interacting with. For physical systems, passivity appears simply as a restatement of energy conservation principle [8]. The concept of passivity being energy related, it is not surprising that bond graph techniques, with their inherent power and energy approach, have been used for passivity based control design (e.g. see [1] [4] or [7]).

In terms of bond graph representation, regular models usually consider power sources as external inputs so that the model junction structure satisfies the continuity of power and energy conservation principle is preserved, provided that the constitutive equations of energy storing elements (C, I) and dissipative elements R satisfy certain conditions widely discussed in [2]. For linear systems considered in this work, those conditions reduce to element parameters being positive or matrices defining multiport fields being positive semidefinite. However, a key feature of many integrated systems is that they contain embedded power sources. The operation of the system relies on the appropriate modulation of the power delivered by the internal sources to perform the required task. For such systems with internal sources, their modulations are performed using active (signal) bonds and physical properties like the energy conservation or the power continuity of the model junction structure, are lost. Also, not considering the control design problem but only models representation and analysis, Beaman and Rosenberg [2] pointed out that *"there are many examples in the literature in which bond graph models for physical systems have been developed with ad hoc procedures such as controlled sources, active bonds and pseudo bonds which in general could violate physical principles."* In their work, they discussed conditions to be imposed on constitutive relationships of individual components for the system to satisfy physical realisability criteria including the passivity property. It is intuitively understandable or it can be shown that if a model consists exclusively of passive components then the model is passive [2] [7]. However, the converse of this statement is not true.

A problem of interest that is considered in the present work is that of determining the conditions under which a system that contains internal active (or nonpassive) elements may be dissipative. Linear bond graph models with individual passive R, I and C elements are investigated with active elements in the model being internal modulated sources that cannot *a priori* be considered as external inputs. The approach will focus on two basic configurations that are widely encountered in control systems or mechatronic devices, namely the cascade interconnection with no loading effect and the closed loop configuration. It is postulated that for more complex systems, these two basic configurations can be recursively used to derive a global passivity condition for the system. The proposed method consists in deriving an equivalent model where external input sources (S_e and S_f) and energy storage elements I and C are identical to the original system but in which

internal modulated sources gains are coupled with the original dissipative field, resulting in a composite R-field that may or may not be truly dissipative. The latter will then be used to determine the conditions for which the system is globally passive.

To further exploit bond graph advantages of representing physical systems layout and flow of energy between components, it will be shown that the proposed equivalent model can be represented as the original model elements (S_e , S_f , R , I and C) that are connected by a so-called *pseudo junction structure* in the sense that it does not ensure the continuity of power. However, the proposed pseudo junction structure highlights a coupling between internal modulation gains and original dissipation parameters and it may be regarded as consisting of a two-layer structure: an *inner* junction structure that satisfies the continuity of power or energy conservation and an *outer* structure in which a power scaling is achieved in relation with the original dissipative elements using power scaling transformers and gyrators introduced in [7].

The paper is organised as follows: after a recall of some passivity concepts and definitions in the context of bond graph modelling, a bond graph pseudo junction structure as an alternative and suitable representation for conservative or nonconservative systems is proposed with a number of examples to explain and illustrate the approach. Important results for two basic configurations, namely the cascade interconnection or closed loop configurations that are common in mechatronic or control systems, are then stated in the following section. A numerical simulation example is presented with some results to illustrate and validate the proposed method and a conclusion section summarises the paper.

Passivity and bond graphs

There are many definitions of passivity in the literature [9]. For n -port systems, which are the most relevant class of systems for our approach, the following definition will be used.

Definition 1. [9] *An n -port is said to be passive if the available energy $E_A(x_0)$, which is the maximum energy that can be extracted from the system for each initial state x_0 , is finite.*

The above definition can be restated using bond graph variables at the ports of the system and the initial state.

Definition 2. [7] *An n -port is passive if for all admissible conjugate pairs (e_i, f_i) , $i = 1, \dots, n$ at the input bonds, and for any initial state x_0 , there exists a constant $c \in \Re$ so that for any time $T \geq 0$,*

$$-\int_0^T \left(\sum_{i=1}^n e_i f_i \right) dt \leq c^2 \quad (1)$$

Eq. (1) expresses the fact that, no matter the power exchanged at the input ports and the time T it takes, the maximum amount of energy that can be extracted from the system (hence the minus sign) is limited by a positive constant c^2 which can be regarded as the initial energy stored in the system and therefore, depends on the initial state only.

From the above definition, it is intuitively clear or it can easily be shown that an n -port bond graph model that consists only of passive R , C and I elements interconnected by junction structure elements (0 , 1 , TF and GY) with no internal active

bonds is passive [7]. The preceding n -port passive model relies on the possibility to treat all the power sources as external inputs at the interface of the n -port system. When the model includes internal sources that are modulated by other variables of the system, it is not possible to treat these sources as external inputs and the fact that the n -port system contains active elements does not necessarily mean that the model cannot be passive. Therefore, knowing that a system that contains active components may be passive, the main question being addressed in the subsequent sections is: *what are the conditions under which a linear system with internal modulated sources can be passive?*

To answer this question, an intuitive idea is to consider that a system which contains active elements will be globally passive if at each instant, the total energy dissipated is greater than the total energy generated internally. For the class of systems considered (with only active elements being internal modulated sources), this implies that a sufficient condition for the system to be passive is that at each instant, the total energy dissipated by the resistive elements is greater than the total energy generated by the internal modulated sources. This leads to the approach of finding an alternative model representation in which the coupling between the internal modulated source gains and the dissipative element parameters will be highlighted and embedded into a composite multiport R-field. The passivity property of the resulting composite multiport R-field will then be used to determine the passivity of the system.

Also, noticing that internal modulated sources break the continuity of power in a junction structure, if the original storage and dissipative elements of the model are maintained in the alternative representation, then its junction structure will also not preserve the continuity of power. For such models, two new bond graph elements were introduced in the context of passification of mechatronic systems in [7]: the power scaling transformer (PTF) and the power scaling gyrator (PGY). These elements behave like regular transformers and gyrators but include an extra scaling between two of the variables leading to the power being scaled by a factor. For a unit transformer ratio and power scaling ρ , the PTF element is shown in Fig. 1 and its defining relationships are given by

$$\begin{aligned} e_2 - e_1 &= 0 \\ f_2 - \rho f_1 &= 0 \end{aligned} \tag{2}$$



Figure 1. Power scaling transformer (PTF) element

This PTF element has the same causal constraints as the regular TF element but the power through it is scaled so that $e_2 f_2 = \rho e_1 f_1$. The PGY element is defined in a similar way. These elements that transfer one power variable with a unit transformer or gyration ratio and scale the conjugate power variable by a factor will appear useful in the representation of pseudo junction structures introduced in the next section as a step toward the development of an alternative representation of models with internal modulated sources. Similar to regular TF and GY bond graph elements, multiport power scaling elements can easily be defined with a vector of power variables transferred as they are and the vector of conjugate power

variables transferred with a scaling factor matrix. These elements will be used in the pseudo junction structure introduced in the next section.

A pseudo junction structure for general bond graph models

Given a regular bond graph model (with no internal active bonds), when integral causality is assigned to the model [5], it can be represented by the junction structure shown in Fig. 2. Elements of the junction structure $S(0, 1, \text{TF}, \text{GY})$ ensure the continuity of power and enforce the constraints among parts of the dynamic system. They instantaneously transfer, convert or distribute power without generation, storage or dissipation. Notations used in Fig. 2 are so that, $x(t) \in \mathfrak{R}^{n \times 1}$ is the state vector associated with I and C elements in integral causality, $z(t) \in \mathfrak{R}^{n \times 1}$ is the co-energy vector composed of effort and flow variables, $D_o(t) \in \mathfrak{R}^{q \times 1}$ and $D_i(t) \in \mathfrak{R}^{q \times 1}$ are vectors which include efforts and flows between the dissipation field R and the junction structure, and $u(t) \in \mathfrak{R}^{m \times 1}$ and $y(t) \in \mathfrak{R}^{p \times 1}$ are the system input and output, respectively. With these definitions, for linear systems, the constitutive equations of the energy storage and the dissipative field are given, respectively, by

$$z(t) = Fx(t) \quad \text{and} \quad D_o(t) = LD_i(t) \quad (3)$$

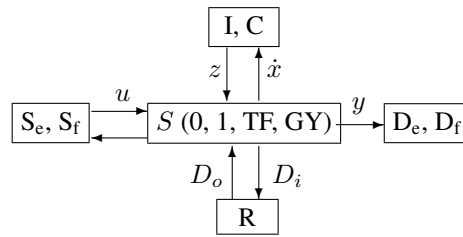


Figure 2. Junction structure of regular bond graph models

The equations for the junction structure are given by:

$$\begin{bmatrix} \dot{x}(t) \\ D_i(t) \\ y(t) \end{bmatrix} = S \begin{bmatrix} z(t) \\ D_o(t) \\ u(t) \end{bmatrix} = \begin{bmatrix} S_{11} & S_{12} & S_{13} \\ S_{21} & S_{22} & S_{23} \\ S_{31} & S_{32} & S_{33} \end{bmatrix} \begin{bmatrix} z(t) \\ D_o(t) \\ u(t) \end{bmatrix} \quad (4)$$

where the junction structure matrix S has a block partition according to the dimensions of $z(t)$, $D_o(t)$ and $u(t)$.

The continuity of power through the regular junction structure implies that the upper left corner part of the junction structure matrix S is skew symmetric (see [5], and [6]) and the following properties hold:

P1 : S_{11} and S_{22} , are skew symmetric.

P2 : $S_{12} = -S_{21}^T$.

In addition, the following property expresses the solvability of the model:

P3 : If the dissipative field is linear, *i.e.*, $D_o(t) = LD_i(t)$, then the model is singular if the matrix $\mathcal{I} - S_{22}L$ is singular.

Therefore, if there are no direct causal paths between R elements, then, $S_{22} = 0$ and the model is nonsingular.

From the constitutive relationships in Eq. (3) and the junction structure relationship in Eq. (4), the state space description of the model can be obtained when it is nonsingular.

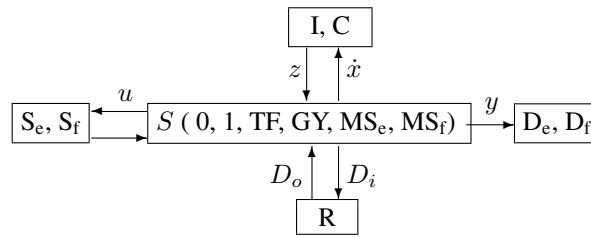


Figure 3. Junction structure with internal modulated sources

The regular junction structure in Fig. 2 treats energy sources as external inputs and therefore ensures that physical principles of energy conservation are satisfied throughout the structure. However, for integrated systems such as mechatronic or control systems with cascade or feedback interconnections, power sources are embedded into the system with their control or modulation achieved through active signal bonds that do not satisfy the continuity of power. For such systems, modulated sources are built into the junction structure as shown in Fig. 3 and properties P1 and P2, highlighting the skew symmetric part of the junction structure, are not satisfied in general. The pseudo junction structure proposed in this section offers an alternative representation for such systems where the conservative part of the junction structure can be separated from the nonconservative part. Internal power generation and dissipation can then be encompassed into a coupled multiport R-field whose properties will be used to determine the passivity of the system.

For matrix dimensions compatibility and invertibility reasons, the construction of the pseudo-junction structure proposed in the following Lemma requires that there is a one-to-one association between each storage and each dissipative element in the model. Although this is a mathematical requirement, its physical justification derives from the fact that models are always approximation to physical systems. Also, augmenting bond graph models with parasitic elements is a well-known technique for various purposes such as, for instance, tearing causal loops for simulation or avoiding dynamic causality in the modelling of switched systems [3]. The one-to-one association between storage and dissipative elements can be achieved by

- i) Connecting high resistors in parallel with each C element or alternatively connecting small capacitors in parallel with each R element as required, and
- ii) Connecting small resistors in series with each storage element I or connecting small inductors in series with each R element, as required.

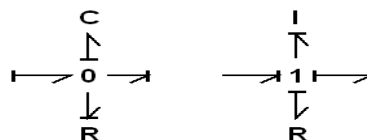


Figure 4. Augmenting the BG model using parasitic elements.

It should be noted that this augmentation is used in the analysis only and has no numerical implication as the relevant parasitic parameters are made to tend either to zero or to infinity, as required, in the end result. The above building proposition is shown in Fig. 4 where a predefined integral causality assignment is realized. So, the strong causal bonds of the energy

storage element impose the causality to all the bonds connected to these junctions and ensures that,

$$e_R = e_C \quad \text{and} \quad f_R = f_I \quad (5)$$

Hence, since these relationships are verified for all pairs of R-C and R-I elements in the augmented bond graph model, submatrices of the junction structure in Eq. (4) are so that,

$$S_{21} = \mathcal{I}_n, \quad S_{22} = 0 \quad \text{and} \quad S_{23} = 0 \quad (6)$$

and property P3 is verified. Also, for a conservative junction structure, owing to property P2, Fig. 4 implies that junction structure submatrix $S_{12} = -\mathcal{I}_n$. However, this property as well as property P1 do not hold for nonconservative junction structures containing internal sources modulated by active bonds. For such systems, an alternative representation is proposed and the construction of the so-called *pseudo junction structure* for an augmented bond graph is stated in the following Lemma.

Lemma 1. *Let a given junction structure S of a bond graph modeling a conservative or a nonconservative LTI system (i.e. including internal modulated sources so that S_{11} is not skew symmetric or the condition $S_{12} = -S_{21}^T$ is not satisfied),*

$$\begin{bmatrix} \dot{x}(t) \\ D_i(t) \\ y(t) \end{bmatrix} = \begin{bmatrix} S_{11} & S_{12} & S_{13} \\ \mathcal{I}_n & 0 & 0 \\ S_{31} & S_{32} & S_{33} \end{bmatrix} \begin{bmatrix} z(t) \\ D_o(t) \\ u(t) \end{bmatrix} \quad (7)$$

that satisfies Eq. (6), where $x(t) \in \mathfrak{R}^{n \times 1}$, $z(t) \in \mathfrak{R}^{n \times 1}$, $D_i(t) \in \mathfrak{R}^{n \times 1}$, $D_o(t) \in \mathfrak{R}^{n \times 1}$, $z(t) = Fx(t)$ and $D_o(t) = LD_i(t)$.

Then, an equivalent pseudo junction inner structure S^i satisfying the power continuity properties P1 and P2 is given by,

$$\begin{bmatrix} \dot{x}(t) \\ D_i(t) \\ y(t) \end{bmatrix} = \begin{bmatrix} 0 & -\mathcal{I}_n & S_{13} \\ \mathcal{I}_n & 0 & 0 \\ S_{31} + S_{32}L & 0 & S_{33} \end{bmatrix} \begin{bmatrix} z(t) \\ \hat{D}_o(t) \\ u(t) \end{bmatrix} \quad (8)$$

where the new coupled multiport R-field is defined by the constitutive relationship,

$$\hat{D}_o(t) = -(S_{11} + S_{12}L)D_i(t) \in \mathfrak{R}^{n \times 1} \quad (9)$$

Moreover, the system is passive if the matrix $\hat{L} := -(S_{11} + S_{12}L)$ is a positive semidefinite matrix.

Proof. From the constitutive equation of the original R-field, $D_o(t) = LD_i(t)$, and the second line of Eq. (7), it follows that $D_o(t) = Lz(t)$. So, substituting $D_o(t) = Lz(t)$ into Eq. (7), and using the definition of the new coupled multiport R-field given in Eq. (9), the result of Eq. (8) is obtained. Clearly, the junction structure in Eq. (8) satisfies properties P1 to P3.

Moreover, the system is passive if, excluding external sources, the elements connected to the conservative pseudo junction inner structure are passive. In this case, energy storage elements are unchanged and assuming these were passive, this property

still holds. As for the new coupled R-field defined by the constitutive Eq. (9), it is truly dissipative if the energy dissipated $D_i^T(t)\hat{D}_o(t) \geq 0$ [2], that is, if

$$-D_i^T(S_{11} + S_{12}L)D_i(t) \geq 0 \quad (10)$$

which is satisfied if $\hat{L} := -(S_{11} + S_{12}L)$ is a positive semidefinite matrix. \square

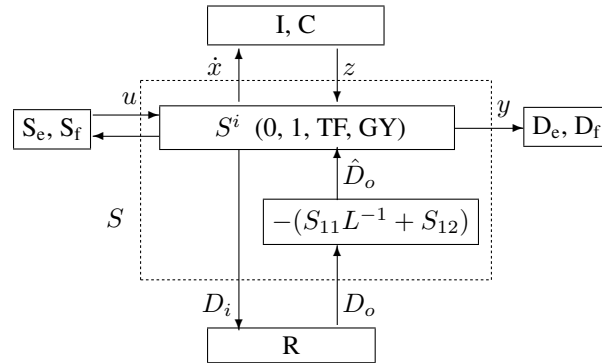


Figure 5. Detailed pseudo junction structure for bond graph model with internal modulated sources

Eqs. (8) and (9) suggest that the pseudo junction structure has the detailed representation given in Fig. 5. This representation clearly shows that the pseudo junction structure consists of an *inner structure* S^i and an *outer structure* S . The inner structure S^i is power conservative, as it contains only 0, 1, TF and GY elements. It also naturally satisfies properties P1 and P2, that is, $\dot{x}^T(t)z(t) + D_i^T(t)\hat{D}_o(t) = 0$ when $u(t) = 0$. The outer structure S does not ensure the continuity of power as expected, that is, in general, $\dot{x}(t)z(t) + D_i(t)D_o(t) \neq 0$ when $u(t) = 0$.

The link between the inner structure S^i and the original dissipative field in the outer structure S , as shown in Fig. 5, has the particularity that while the vector of power variables D_i is transferred without any change, its conjugate D_o is scaled by a matrix factor $S_{KD} := -(S_{11}L^{-1} + S_{12})$ into \hat{D}_o . This is typical of power scaling elements introduced in [7] and recalled in the previous section. Therefore, the pseudo-junction structure introduced in Lemma 1 and shown in Fig. 5 can be used to provide an equivalent bond graph model as shown in Fig. 6. In this alternative representation, the multiport power scaling elements PTF and PGY have a scaling factor matrix $S_{KD} := -(S_{11}L^{-1} + S_{12})$ which involve a coupling between the existing modulated sources gains included in the submatrices S_{11} and S_{12} and the original dissipative field parameters in matrix L .

Remark 1: For regular bond graph models (with no internal modulated sources), the effect of the scaling matrix S_{KD} reduces, as expected, to a unit power scaling factor in the sense that $D_i^T\hat{D}_o = D_i^TD_o$. The proof for this is provided in Appendix 1. For such models, the alternative pseudo junction structure representation provides a model in which all the dissipative fields are encompassed into a single multiport R-field.

Before generalising the method to usual configurations present in mechatronic or control systems, the following two examples show simple applications of Lemma 1 to a cascade interconnections with no loading effect and a closed-loop configuration. A third example illustrates the effect of augmenting the model with parasitic elements. In each case, the equivalent bond graph model with power scaling elements is given and the passivity property of the model is discussed.

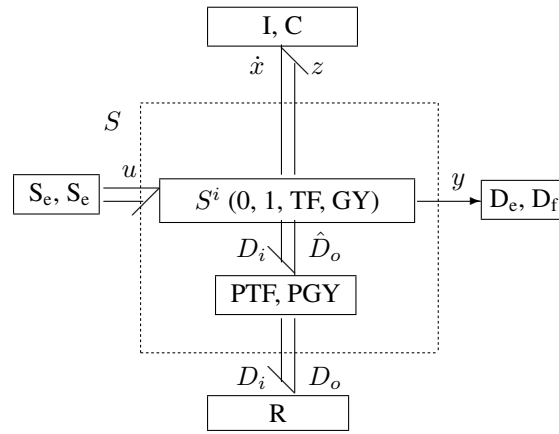


Figure 6. Detailed equivalent bond graph with pseudo-junction structure including power scaling elements

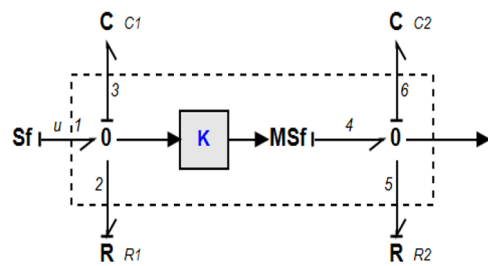


Figure 7. Bond graph of a cascade interconnection of R-C circuits

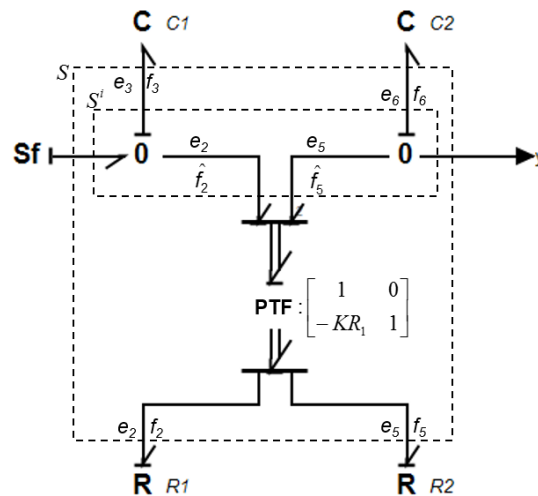


Figure 8. Equivalent model of the system in Fig. 7 using the pseudo-junction structure and power scaling element

The following example is an illustration of how Lemma 1 can be applied to the equivalent representation of a cascade interconnection of systems.

Example 1. Let two R-C circuits interconnected in cascade as shown in Fig. 7, where the dotted box highlights the junction structure with internal modulated source. In this figure, the modulated source of flow supplying the second R-C circuit is internal to the system and therefore the continuity of power is not satisfied. The problem in this case is to find an equivalent model representation using the proposed pseudo junction structure and to determine the conditions for which the system is passive.

Element constitutive relationships are: $e_3 = (1/C_1)q_3$, $e_5 = (1/C_2)q_5$, $f_2 = (1/R_1)e_2$ and $f_5 = (1/R_2)e_5$. And, with the modulated source so that $f_4 = Ke_3$, where K is the modulation gain, the equations at various nodes of the model give the following junction structure equation for the cascaded system,

$$\begin{bmatrix} f_3 \\ f_6 \\ e_2 \\ e_5 \\ e_6 \end{bmatrix} = \left[\begin{array}{cc|cc|c} 0 & 0 & -1 & 0 & 1 \\ K & 0 & 0 & -1 & 0 \\ \hline 1 & 0 & 0 & 0 & 0 \\ 0 & 1 & 0 & 0 & 0 \\ \hline 0 & 1 & 0 & 0 & 0 \end{array} \right] \begin{bmatrix} e_3 \\ e_6 \\ f_2 \\ f_5 \\ f_1 \end{bmatrix} \quad (11)$$

The junction structure equation given by Eq. (11) does not obviously satisfy the continuity of power as the submatrix S_{11} is not skew symmetric (property P1 is not satisfied). Using Lemma 1, an equivalent power conservative *inner* junction structure S^i is given by

$$\begin{bmatrix} f_3 \\ f_6 \\ e_2 \\ e_5 \\ e_6 \end{bmatrix} = \left[\begin{array}{cc|cc|c} 0 & 0 & -1 & 0 & 1 \\ 0 & 0 & 0 & -1 & 0 \\ \hline 1 & 0 & 0 & 0 & 0 \\ 0 & 1 & 0 & 0 & 0 \\ \hline 0 & 1 & 0 & 0 & 0 \end{array} \right] \begin{bmatrix} e_3 \\ e_6 \\ \hat{f}_2 \\ \hat{f}_5 \\ f_1 \end{bmatrix} \quad (12)$$

with the scaling matrix in the *outer* structure S defined by

$$\begin{bmatrix} \hat{f}_2 \\ \hat{f}_5 \end{bmatrix} = \begin{bmatrix} 1 & 0 \\ -KR_1 & 1 \end{bmatrix} \begin{bmatrix} f_2 \\ f_5 \end{bmatrix} \quad (13)$$

Combining Eq. (13) with the defining equations of the R-elements gives the multiport coupled R-field constitutive relationship in the cascade interconnection,

$$\begin{bmatrix} \hat{f}_2 \\ \hat{f}_5 \end{bmatrix} = \begin{bmatrix} 1/R_1 & 0 \\ -K & 1/R_2 \end{bmatrix} \begin{bmatrix} e_2 \\ e_5 \end{bmatrix} \quad (14)$$

From the above results, an equivalent bond graph model of the cascade interconnection of R-C circuits (Fig. 7) is shown in Fig. 8 using a pseudo junction structure (with a multiport power scaling transformer). The passivity of the cascaded system can be determined from the positive semidefiniteness of the matrix defining the multiport coupled R-field in Eq. (14). In this case, the positive semidefiniteness of the symmetric part of this matrix shows that the system is passive if $K \leq 2/\sqrt{R_1 R_2}$ and active otherwise.

Remark 2: For this simple example, the constitutive matrix in Eq. (14), defining the multiport coupled R-field whose positive semidefiniteness determines the passivity of the system, can also be obtained by writing down that the total power

dissipated by resistances R_1 and R_2 should be higher than the power generated by the internal modulated source MS_f , that is, $e_2 f_2 + e_5 f_5 \geq e_4 f_4$ using bonds indexing in Fig. 7. The proof of this result is provided in Appendix 2.

This remark highlights the underlying principle of the passivity analysis method proposed in this paper and the aim is to develop a systematic approach for the most common configurations. The following example applies Lemma 1 to the equivalent representation and analysis of a closed-loop RC-circuit.

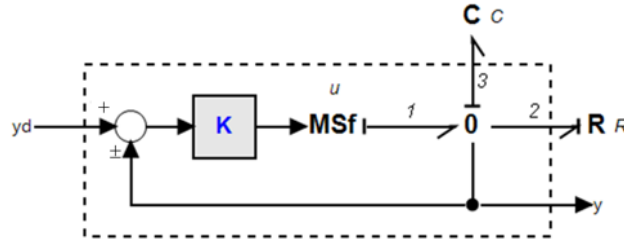


Figure 9. Bond graph of a R-C circuit with a feedback interconnection.

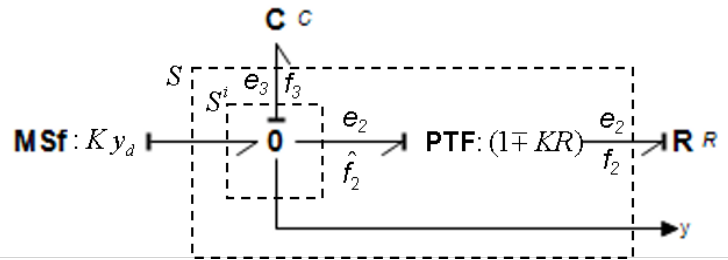


Figure 10. Equivalent model of the closed-loop R-C circuit using power scaling element

Example 2. Consider the R-C circuit with a positive or negative feedback loop as shown in Fig. 9, where the dotted box highlights the junction structure with internal modulated source. The junction structure equation for this system is given by

$$\begin{bmatrix} f_3 \\ e_2 \\ y \end{bmatrix} = \begin{bmatrix} \pm K & -1 & K \\ 1 & 0 & 0 \\ 1 & 0 & 0 \end{bmatrix} \begin{bmatrix} e_3 \\ f_2 \\ y_d \end{bmatrix} \quad (15)$$

where K is the gain of the modulated source of flow and the constitutive equations of the external elements are $f_2 = (1/R)e_2$ and $e_3 = (1/C)q_3$. The continuity of power is obviously not satisfied here and the junction structure submatrix $S_{11} = \pm K$ is not skew symmetric (Property P1 not satisfied).

Applying Lemma 1 leads to the equivalent pseudo junction inner structure

$$\begin{bmatrix} f_3 \\ e_2 \\ y \end{bmatrix} = \begin{bmatrix} 0 & -1 & K \\ 1 & 0 & 0 \\ 1 & 0 & 0 \end{bmatrix} \begin{bmatrix} e_3 \\ \hat{f}_2 \\ y_d \end{bmatrix} \quad (16)$$

This pseudo junction structure is power conservative, and the new coupled R-field constitutive relationship defined by Eq. (9) is given by

$$\hat{f}_2 = -(\pm K - 1/R) e_2 \quad (17)$$

An alternative view of the system using the detailed pseudo junction structure in Fig. 5 is to consider that in the outer structure, there is a power scaling transformation with the scaling factor $S_{KD} := -(\pm KR - 1)$ in the link to the R-field so that $\hat{f}_2 = -(\pm KR - 1) f_2$. A representation of the system using a power scaling transformer is shown in Fig. 10. From the resulting coupled R-field constitutive relationship in Eq. (17), the above R-C closed loop circuit is always passive for negative feedback. However, for positive feedback the system is passive only if $K \leq 1/R$ and active otherwise. A physical interpretation in this case is that, for negative feedback, both the internal modulated source and the R-element contribute to the dissipation of energy for any value of K positive, whereas for positive feedback, the balance between the energy generated by the internal source and the energy dissipated by the R-element results in net dissipation only when $K \leq 1/R$.

The above two examples cover the case of systems with internal modulated source. A requirement for the application of Lemma 1 is that the model has an appropriate one-to-one association of R-elements with storage I- or C-elements as shown in Fig. 4. As previously explained, this can be achieved by augmenting the bond graph with parasitic elements of adequate order of magnitude. The following example discusses the effect of such augmentation on a bond graph model and shows how Lemma 1 can be applied to a regular bond graph model (with no active bonds) to obtain an alternative model representation.

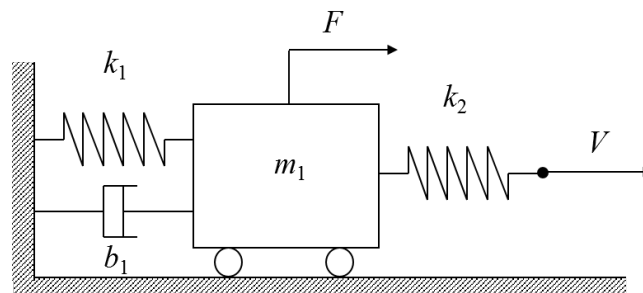


Figure 11. A two-port mechanical system

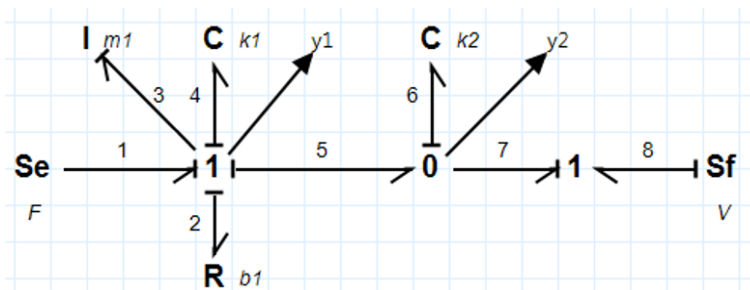


Figure 12. Bond graph model of the mechanical system in Fig. 11

Example 3. Consider the mechanical system shown in Fig. 11, where m_1 , b_1 , and k_i , $i = 1, 2$, are the mass, the damping coefficient and the stiffness parameters, respectively. Force $e_1(t)$ and velocity $f_8(t)$ are inputs applied to the system and the outputs are the velocity $y_1(t)$ of the mass and the spring force $y_2(t)$ as indicated. The bond graph model of this system is shown in Fig. 12. In order to apply Lemma 1, ensuring a square nonsingular junction structure submatrix S_{21} , the model is

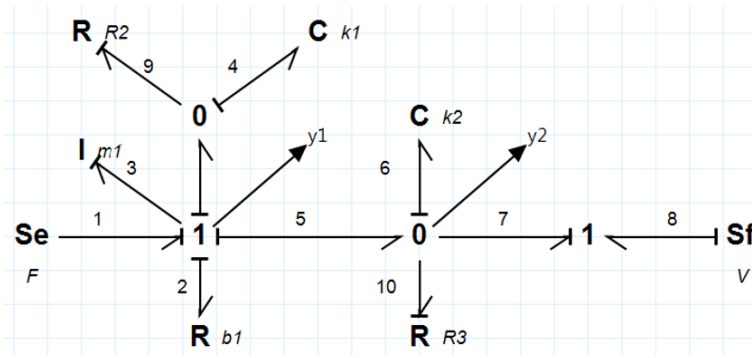


Figure 13. Augmented bond graph of the model in Fig. 12

initially augmented with high resistors R_2 and R_3 as show in Fig. 13. And the junction structure equation of this augmented model is,

$$\begin{bmatrix} \dot{x}(t) \\ D_i(t) \\ y(t) \end{bmatrix} = \begin{bmatrix} S_{11} & -\mathcal{I}_3 & S_{13} \\ \mathcal{I}_3 & 0 & 0 \\ S_{31} & 0 & 0 \end{bmatrix} \begin{bmatrix} z(t) \\ D_o(t) \\ u(t) \end{bmatrix} \quad (18)$$

where $S_{11} = \begin{bmatrix} 0 & -1 & -1 \\ 1 & 0 & 0 \\ 1 & 0 & 0 \end{bmatrix}$, $S_{13} = \begin{bmatrix} 1 & 0 \\ 0 & 0 \\ 0 & -1 \end{bmatrix}$, $S_{31} = \begin{bmatrix} 1 & 0 & 0 \\ 0 & 0 & 1 \end{bmatrix}$, $\dot{x}(t) = [\dot{p}_3 \quad \dot{q}_4 \quad \dot{q}_6]^T$,

$$D_i(t) = [f_2 \quad e_9 \quad e_{10}]^T, \quad y(t) = [f_3 \quad e_6]^T, \quad z(t) = [f_3 \quad e_4 \quad e_6]^T, \quad D_o(t) = [e_2 \quad f_9 \quad f_{10}]^T \quad \text{and}$$

$$u(t) = [e_1 \quad f_8]^T.$$

From Lemma 1, an equivalent pseudo junction inner structure S^i satisfying the energy conservation properties P1 and P2 is,

$$\begin{bmatrix} \dot{x}(t) \\ D_i(t) \\ y(t) \end{bmatrix} = \begin{bmatrix} 0 & -\mathcal{I}_3 & S_{13} \\ \mathcal{I}_3 & 0 & 0 \\ S_{31} & 0 & 0 \end{bmatrix} \begin{bmatrix} z(t) \\ \hat{D}_o(t) \\ u(t) \end{bmatrix} \quad (19)$$

where, according to Eq. (9), the new coupled multiport R-field constitutive equation is

$$\hat{D}_o(t) = \begin{bmatrix} b_1 & 1 & 1 \\ -1 & \frac{1}{R_2} & 0 \\ -1 & 0 & \frac{1}{R_3} \end{bmatrix} D_i(t) \quad (20)$$

In this case, it is easy to see that the multiport coupled R-field defining matrix in Eq. (20) can be decomposed into a skew symmetric matrix (having zero contribution to the dissipation of energy) and a diagonal matrix $diag\{b_1, 1/R_2, 1/R_3\}$ whose terms are the resistances and conductances of the R-elements. Moreover as the parasitic parameters R_2 and R_3 tend to infinity, the associated terms in the matrix tend to zero, meaning that only the original system R-element really contributes to the energy dissipation and therefore to the passivity property of the system.

Applying Lemma 1 to a regular bond graph, as shown in this example, has the effect of encompassing all dissipative elements (including the parasitic ones) into a multiport coupled R-element as shown in the equivalent bond graph of the augmented system in Fig. 14. For a regular bond graph, the passivity is obvious and this alternative representation does not have a major interest. However, for systems with internal modulated sources, Lemma 1 provides an alternative representation where all dissipation and internal power generation are included into an overall coupled multiport R-field. The balance of dissipation and internal generation is then expressed in the constitutive equation of this composite element and therefore determines the passivity property of the overall system.

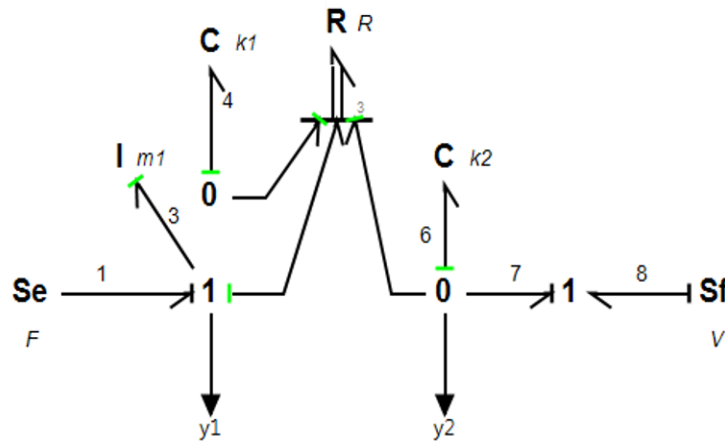


Figure 14. Alternative representation of the model in Fig. 13 (with multiport R-field defined by Eq. 20).

In the following sections, the preliminary examples are generalised and the proposed pseudo junction structure is applied to the passivity analysis of some common configurations that appear in control systems, namely the cascade and the feedback interconnections.

Passivity analysis of systems interconnected in cascade

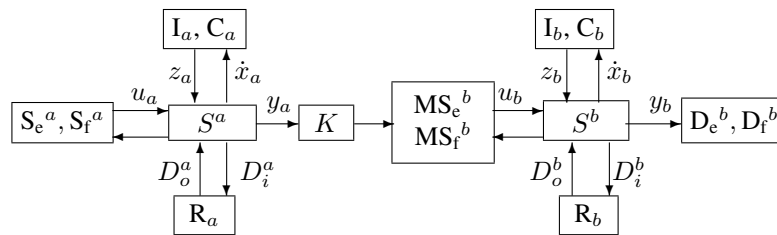


Figure 15. Bond graph model of systems interconnected in cascade (with no loading effect)

The aim is to get an alternative but equivalent representation for given systems represented by bond graphs with junction structures S^a and S^b interconnected in cascade as shown in Fig. 15. It is assumed that S^b does not have a loading effect on S^a . So, both models are connected by active (signal) bonds that modulate sources of effort MS_e^b or flow MS_f^b . These sources usually model a fixed ideal source connected in series with a variable resistor that is adjusted by an active bond. Due to this signal connection, the junction structure of the overall system does not conserve energy. However, in what follows, it is

shown that it is possible to develop an alternative model representation using the pseudo junction structure introduced in the previous section with an *inner* structure that ensures the continuity of power and an *outer* structure in which there is a power scaling conversion. The following Theorem states its construction.

Theorem 1. *Let two junction structures S^a and S^b of bond graphs modelling conservative or nonconservative LTI systems, and given by*

$$\begin{bmatrix} \dot{x}_a(t) \\ D_i^a(t) \\ y_a(t) \end{bmatrix} = \begin{bmatrix} S_{11}^a & S_{12}^a & S_{13}^a \\ \mathcal{I}_{n_a} & 0 & 0 \\ S_{31}^a & S_{32}^a & S_{33}^a \end{bmatrix} \begin{bmatrix} z_a(t) \\ D_o^a(t) \\ u_a(t) \end{bmatrix}, \quad (21)$$

and

$$\begin{bmatrix} \dot{x}_b(t) \\ D_i^b(t) \\ y_b(t) \end{bmatrix} = \begin{bmatrix} S_{11}^b & S_{12}^b & S_{13}^b \\ \mathcal{I}_{n_b} & 0 & 0 \\ S_{31}^b & S_{32}^b & S_{33}^b \end{bmatrix} \begin{bmatrix} z_b(t) \\ D_o^b(t) \\ u_b(t) \end{bmatrix} \quad (22)$$

that satisfy Eq. (6), where $x_a(t) \in \mathfrak{R}^{n_a \times 1}$, $z_a(t) = F_a x_a \in \mathfrak{R}^{n_a \times 1}$, $D_i^a(t) \in \mathfrak{R}^{n_a \times 1}$, $D_o^a(t) = L_a D_i^a(t) \in \mathfrak{R}^{n_a \times 1}$, $x_b(t) \in \mathfrak{R}^{n_b \times 1}$, $z_b(t) = F_b x_b(t) \in \mathfrak{R}^{n_b \times 1}$, $D_i^b(t) \in \mathfrak{R}^{n_b \times 1}$ and $D_o^b(t) = L_b D_i^b(t) \in \mathfrak{R}^{n_b \times 1}$.

Suppose that S^a and S^b are interconnected in cascade with no loading effect so that $u_b(t) = K y_a(t)$, where K is a nonsingular matrix composed of the modulating gains of MS_e^b and MS_f^b .

Then, a pseudo junction inner structure S_{ab}^i for the cascade interconnection, satisfying the energy conservation properties P1 and P2 is,

$$\begin{bmatrix} \dot{x}(t) \\ D_i(t) \\ y_b(t) \end{bmatrix} = \begin{bmatrix} 0 & -\mathcal{I}_{n_a+n_b} & S_{13} \\ \mathcal{I}_{n_a+n_b} & 0 & 0 \\ S_{31} + S_{32}L & 0 & S_{33} \end{bmatrix} \begin{bmatrix} z(t) \\ \hat{D}_o(t) \\ u_a(t) \end{bmatrix} \quad (23)$$

where $\dot{x}(t) := \begin{bmatrix} \dot{x}_a^T(t) & \dot{x}_b^T(t) \end{bmatrix}^T$, $D_i(t) := \begin{bmatrix} (D_i^a(t))^T & (D_i^b(t))^T \end{bmatrix}^T$, $z(t) := \begin{bmatrix} z_a^T(t) & z_b^T(t) \end{bmatrix}^T \in \mathfrak{R}^{(n_a+n_b) \times 1}$, $\hat{D}_o(t) := \begin{bmatrix} (\hat{D}_o^a(t))^T & (\hat{D}_o^b(t))^T \end{bmatrix}^T \in \mathfrak{R}^{(n_a+n_b) \times 1}$,

$$S_{13} := \begin{bmatrix} S_{13}^a \\ S_{13}^b K S_{33}^a \end{bmatrix}, \quad S_{31} := \begin{bmatrix} S_{33}^b K S_{31}^a & S_{31}^b \end{bmatrix}, \quad (24)$$

$$S_{32} := \begin{bmatrix} S_{33}^b K S_{32}^a & S_{32}^b \end{bmatrix}, \quad S_{33} := S_{33}^b K S_{33}^a, \quad (25)$$

And the multiport coupled R-field constitutive relationship is,

$$\hat{D}_o(t) = L_{ab} D_i(t) \quad (26)$$

where,

$$L_{ab} := - \begin{bmatrix} S_{11}^a + S_{12}^a L_a & 0 \\ S_{13}^b K (S_{31}^a + S_{32}^a L_a) & S_{11}^b + S_{12}^b L_b \end{bmatrix} \quad (27)$$

Moreover, the system is passive if L_{ab} is a positive semidefinite matrix.

Proof. The continuity of power is not ensured when systems are interconnected with no loading effect using active bonds as shown in Fig. 15. Since $u_b(t) = Ky_a(t)$, expanding the expression of the output y_a from the junction structure S^a (third line of Eq. (21)) and substituting the resulting expression of u_b into Eq. (22) leads, after concatenation of both sets of equations, to the following overall junction structure S equations,

$$\begin{aligned} \dot{x}(t) &= S_{11}z(t) + S_{12}D_o(t) + S_{13}u_a(t) \\ D_i(t) &= z(t) \\ y_b(t) &= S_{31}z(t) + S_{32}D_o(t) + S_{33}u_a(t) \end{aligned} \quad (28)$$

where variables x , z , D_o and D_i are formed by the concatenation of relevant variables of both systems and

$$\begin{aligned} S_{11} &:= \begin{bmatrix} S_{11}^a & 0 \\ S_{13}^b K S_{31}^a & S_{11}^b \end{bmatrix}, & S_{12} &:= \begin{bmatrix} S_{12}^a & 0 \\ S_{13}^b K S_{32}^a & S_{12}^b \end{bmatrix}, & S_{13} &:= \begin{bmatrix} S_{13}^a \\ S_{13}^b K S_{33}^a \end{bmatrix}, \\ S_{31} &:= \begin{bmatrix} S_{33}^b K S_{31}^a & S_{31}^b \end{bmatrix}, & S_{32} &:= \begin{bmatrix} S_{33}^b K S_{32}^a & S_{32}^b \end{bmatrix}, & S_{33} &:= S_{33}^b K S_{33}^a \end{aligned} \quad (29)$$

The overall junction structure relationship in Eq. (28) with submatrices given by Eq. (29) does not satisfy the structural properties (P1 and P2) of power continuity when $K \neq 0$, that is, S_{11} is not skew symmetric and $S_{12}^T \neq -S_{21}$ in general. Hence, applying Lemma 1 to the cascaded junction structure of Eq. (28), the result of Eq. (23) in the Theorem follows, where the constitutive relationship of the coupled multiport R-field is,

$$\hat{D}_o(t) := -(S_{11} + S_{12}L_{ab})D_i(t) \quad (30)$$

with $L_{ab} := \text{diag}\{L_a, L_b\}$.

Then, substituting submatrix definitions S_{11} and S_{12} from Eq. (29) into Eq. (30), the multiport coupled R-field matrix of Eq. (27) is obtained and the passivity condition follows. \square

The above proof of Theorem 1 first realises the interconnection of the systems and then applies Lemma 1 to the resulting cascaded junction structure. An alternative approach, leading to the same result, can be to apply Lemma 1 initially to systems S^a and S^b , and then apply Lemma 1 again after the cascade interconnection of resulting pseudo junction structures.

Remark 3: The triangular structure of the multiport coupled R-field matrix given in Eq. (27) and shown in Fig. 16, confirms that the subsystem S^a is not affected in the interconnection with no loading effect and also indicates, as expected, that if the

first system is not passive, then the interconnected system will not be passive.

Theorem 1 suggests that the cascaded system interconnection can be represented by an equivalent *inner* junction structure described by Eq. (23) that is energy conservative and a multiport coupled R-field with the constitutive relationship given by Eq. (26). However, if the original dissipative elements of the system are to be maintained in the new representation, a detailed equivalent junction structure of the cascade interconnection shown in Fig. 16 can be represented using the expanded expression of \hat{D}_o from Eq. (26). In Fig. 16, the inner junction structure S_{ab}^i is conservative and the matrices S_{KD}^a , S_{KD}^a and S_{KD}^{ab} express the coupling between internal sources and dissipative elements and are defined as:

- $S_{KD}^a := -(S_{11}^a L_a^{-1} + S_{12}^a)$ and $S_{KD}^b := -(S_{11}^b L_b^{-1} + S_{12}^b)$ which are associated with the distinct couplings of internal power generation and dissipation in the individual subsystems S^a and S^b respectively,
- $S_{KD}^{ab} := -S_{13} K (S_{13}^a L_a^{-1} + S_{32}^a)$ which expresses the cross-couplings between the two subsystems S^a and S^b . In particular, it shows how the dissipative field L_a and the modulation gain matrix K affect the dissipation in subsystem S^b .

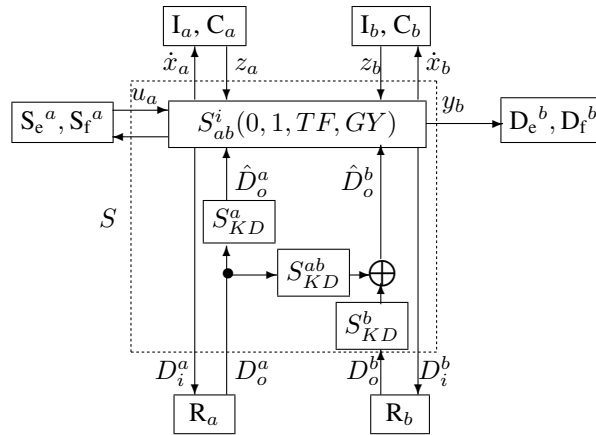


Figure 16. Detailed equivalent junction structure of systems interconnected in cascade

Passivity analysis of closed-loop systems

The following Theorem presents the construction of a pseudo junction structure for a given system represented by a bond graph in a closed loop configuration as shown in Fig. 17. To keep the result general and applicable to various mechatronic system configurations, both positive and negative feedback possibilities are considered although in general, only negative feedback will apply in the context of control systems.

Theorem 2. *Let a junction structure S of a bond graph modelling a conservative or nonconservative LTI system,*

$$\begin{bmatrix} \dot{x}(t) \\ D_i(t) \\ y(t) \end{bmatrix} = \begin{bmatrix} S_{11} & S_{12} & S_{13} \\ \mathcal{I}_n & 0 & 0 \\ S_{31} & S_{32} & S_{33} \end{bmatrix} \begin{bmatrix} z(t) \\ D_o(t) \\ u(t) \end{bmatrix}, \quad (31)$$

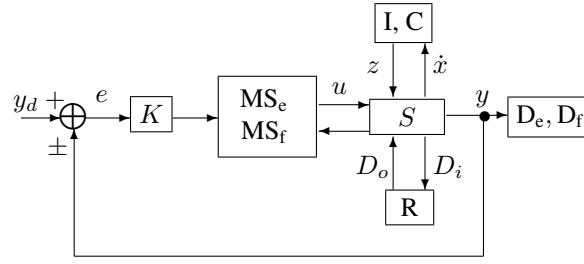


Figure 17. System in a closed loop configuration

that satisfy Eq. (6), where $x(t) \in \mathfrak{R}^{n \times 1}$, $z(t) = Fx(t) \in \mathfrak{R}^{n \times 1}$, $D_i(t) \in \mathfrak{R}^{n \times 1}$, $D_o(t) = LD_i(t) \in \mathfrak{R}^{n \times 1}$,

Suppose that the system is in a closed loop configuration as shown in Fig. 17, with $u(t) = K(y_d(t) \pm y(t))$, where K is a nonsingular matrix composed of the control gains.

Then, an inner junction structure S_{cl}^i for the closed loop system, satisfying the energy conservation properties P1 and P2 is,

$$\begin{bmatrix} \dot{x}(t) \\ D_i(t) \\ y(t) \end{bmatrix} = \begin{bmatrix} 0 & -\mathcal{I}_n & S_{13}NK \\ \mathcal{I}_n & 0 & 0 \\ (\mathcal{I} + S_{33}K)^{-1} \hat{S}_{31} & 0 & S_{33}NK \end{bmatrix} \begin{bmatrix} z(t) \\ \hat{D}_{ocl}(t) \\ y_d(t) \end{bmatrix} \quad (32)$$

with the multiport coupled R-field constitutive relationship defined by,

$$\hat{D}_{ocl}(t) := \left(\hat{L} \mp S_{13}NK \hat{S}_{31} \right) D_i(t) \quad (33)$$

where $\hat{L} := -(S_{11} + S_{12}L)$, $\hat{S}_{31} := S_{31} + S_{32}L$ and $N := (\mathcal{I}_n \mp KS_{33})^{-1}$,

Moreover, the closed loop system is passive if the closed loop multiport R-field matrix $\hat{L}_{cl} := \hat{L} \mp S_{13}NK \hat{S}_{31}$ is a positive semidefinite matrix.

Proof. The proof of this Theorem can be done in two ways that are equivalent. Lemma 1 can first be applied to the junction structure of the open loop system and then reapplied a second time to the closed loop configuration. Or alternatively, the closed loop junction structure equations can first be derived and Lemma 1 can then be applied once on the resulting junction structure. The first method is shown here. Applying Lemma 1 to the open loop configuration of the system in Fig. 17 leads to the equivalent inner junction structure

$$\begin{bmatrix} \dot{x}(t) \\ D_i(t) \\ y(t) \end{bmatrix} = \begin{bmatrix} 0 & -\mathcal{I}_n & S_{13} \\ \mathcal{I}_n & 0 & 0 \\ \hat{S}_{31} & 0 & S_{33} \end{bmatrix} \begin{bmatrix} z(t) \\ \hat{D}_o(t) \\ u(t) \end{bmatrix} \quad (34)$$

where $\hat{S}_{31} = S_{31} + S_{32}L$ and the open loop system multiport R-field is defined by

$$\hat{D}_o(t) := -(S_{11} + S_{12}L)D_i(t) \in \mathfrak{R}^{n \times 1} \quad (35)$$

From the closed loop feedback equation $u = K(y_d \pm y)$ and the third line of Eq. (34),

$$u(t) = NK \left(y_d(t) \pm \hat{S}_{31} z(t) \right) \quad (36)$$

where $N := (\mathcal{I} \mp KS_{33})^{-1}$

Since, $(\mathcal{I} \pm S_{33}NK) \hat{S}_{31} = \left[\mathcal{I} \pm (\mathcal{I} \mp S_{33}K)^{-1} S_{33}K \right] \hat{S}_{31} = (\mathcal{I} \mp S_{33}K)^{-1} \hat{S}_{31}$, then, from Eqs. (34) and (36), the junction structure for the closed loop system is,

$$\begin{bmatrix} \dot{x}(t) \\ D_i(t) \\ y(t) \end{bmatrix} = \begin{bmatrix} \pm S_{13}NK \hat{S}_{31} & -\mathcal{I}_n & S_{13}NK \\ \mathcal{I}_n & 0 & 0 \\ (\mathcal{I} \mp S_{33}K)^{-1} \hat{S}_{31} & 0 & S_{33}NK \end{bmatrix} \begin{bmatrix} z(t) \\ \hat{D}_o(t) \\ y_d(t) \end{bmatrix} \quad (37)$$

Reapplying Lemma 1 to the junction structure of Eq. (37) gives the equivalent inner junction structure

$$\begin{bmatrix} \dot{x}(t) \\ D_i(t) \\ y(t) \end{bmatrix} = \begin{bmatrix} 0 & -\mathcal{I}_n & S_{13}NK \\ \mathcal{I}_n & 0 & 0 \\ (\mathcal{I} \mp S_{33}K)^{-1} \hat{S}_{31} & 0 & S_{33}NK \end{bmatrix} \begin{bmatrix} z(t) \\ \hat{D}_{ocl}(t) \\ u(t) \end{bmatrix} \quad (38)$$

with the new multiport closed loop coupled R-field defined by $\hat{D}_{ocl}(t) := -(\pm S_{13}NK \hat{S}_{31} - \hat{L})D_i(t)$.

The passivity condition follows directly from the positive semidefiniteness of the matrix $\hat{L}_{cl} := \hat{L} \mp S_{13}NK \hat{S}_{31}$. \square

Similar to the cascade interconnection, using the constitutive equation of the multiport R-field, a detailed junction structure for the closed loop configuration can be described as shown in Fig. 18 if the original elements of the system are to be maintained. The inner structure S_{cl}^i is conservative and the matrix S_{KD}^{ol} expresses the coupling between internal sources and dissipative elements in open loop while S_{KD}^{cl} expresses additional coupling due to the feedback connection in closed loop. These matrices are defined as:

$$S_{KD}^{ol} := -(S_{11}L^{-1} + S_{12}) \quad \text{and} \quad S_{KD}^{cl} := -S_{13}NK \hat{S}_{31}L^{-1} = -S_{13}(\mathcal{I}_n \mp KS_{33})^{-1}K(S_{31}L^{-1} + S_{32}) \quad (39)$$

Simulation results and discussion

The application of the method developed in the preceding sections and the physical interpretation of the passivity property are presented in this section using numerical simulations. For this, the two-port mechanical system (Fig. 11) in Example 3 is now considered in a closed-loop configuration (Fig. 19) so that $u = K(y_d \pm y)$ with the modulating gain matrix given by

$$K = \begin{bmatrix} K_{11} & K_{12} \\ K_{21} & K_{22} \end{bmatrix} \quad (40)$$

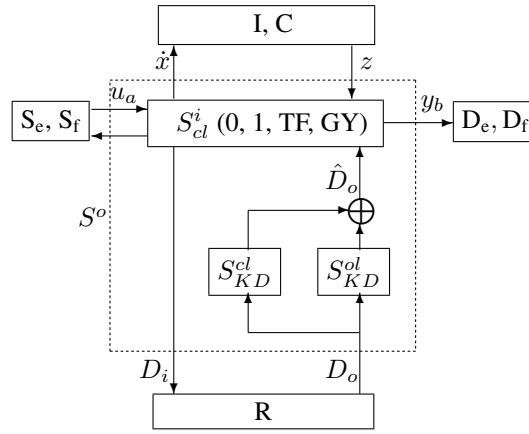


Figure 18. Equivalent junction structure of a closed loop configuration

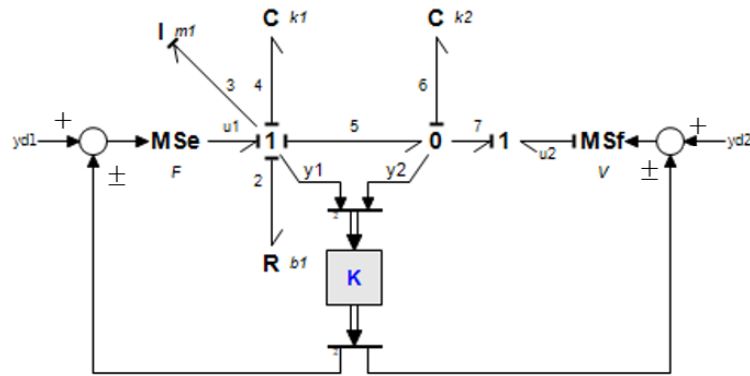


Figure 19. Closed loop configuration of the mechanical system in Fig. 11

In Example 3, the dissipative field of the (open-loop) augmented bond graph model is given by Eq. (20). Substituting this matrix in Eq. (33) of Theorem 2 and using the relevant submatrices of the model junction structure give the multiport coupled R-field constitutive matrix of the closed-loop configuration,

$$\hat{L}_{cl} = \begin{bmatrix} b_1 \mp K_{11} & 1 & 1 \mp K_{12} \\ -1 & \frac{1}{R_2} & 0 \\ -1 \pm K_{21} & 0 & \frac{1}{R_3} \pm K_{22} \end{bmatrix} \quad (41)$$

The positive semidefiniteness of the matrix in Eq. (41) determines the passivity of the closed-loop system. For this, Sylvester's criterion is applied to the symmetric part of the matrix \hat{L}_{cl} defined as

$$\text{sym}\{\hat{L}_{cl}\} := \frac{1}{2}(\hat{L}_{cl} + \hat{L}_{cl}^T) = \begin{bmatrix} b_1 \mp K_{11} & 0 & \frac{1}{2}(\mp K_{12} \pm K_{21}) \\ 0 & \frac{1}{R_2} & 0 \\ \frac{1}{2}(\mp K_{12} \pm K_{21}) & 0 & \frac{1}{R_3} \pm K_{22} \end{bmatrix} \quad (42)$$

As the parasitic elements R_2 and R_3 tend to infinity,

- for positive feedback, the passivity conditions are

$$K_{11} \leq b_1, \quad |K_{21} - K_{12}| \leq 2\sqrt{(b_1 - K_{11})K_{22}} \quad \text{and} \quad K_{22} \geq 0 \quad (43)$$

- and for negative feedback, the passivity conditions are

$$\text{Any } K_{11} \geq 0, \quad K_{21} = K_{12} \quad \text{and} \quad K_{22} = 0 \quad (44)$$

Some numerical simulations are carried out to validate the above theoretical results. Model parameters and initial conditions used in the simulation are summarised in Table 1.

Table 1. System parameters and initial conditions

	mass m_1	stiffness k_1	stiffness k_2	damping b_1
Parameters	$m_1 = 1 \text{ kg}$	$k_1 = 100 \text{ N/s}$	$k_2 = 100 \text{ N/s}$	$b_1 = 1 \text{ Ns/m}$
Initial conditions	$v_o = 1 \text{ m/s}$	$x_{01} = 0.1 \text{ m}$	$x_{02} = 0.1 \text{ m}$	-

With the above parameters and initial state, the total energy initially stored in the system is $E_o = 1.5 \text{ J}$. This quantity represents the maximum amount of energy that can be extracted from the system if it is passive.

For conciseness sake, only the positive feedback configuration is considered and conditions stated by Eq. (43) are required for the system to be passive. Without loss of generality, demand inputs y_{d1} and y_{d2} are set to zero and the investigation is concerned with the effect of the modulating gains ($K_{ij}; i, j = 1, 2$) on the passivity of the closed-loop system according to the conditions of Eq. (43). From these passivity conditions, three sets of simulations centered around the first condition ($K_{11} \leq b_1$) are run to illustrate the energetic behaviour of the system in the following situations:

- a nonpassive (or active) case when $K_{11} > b_1$,
- the limit of passivity when $K_{11} = b_1$ and $K_{21} = K_{12}$,
- and a passive (or dissipative) case when $K_{11} < b_1$ and $|K_{21} - K_{12}| \leq 2\sqrt{(b_1 - K_{11})K_{22}}$.

The choice of modulating gains $K_{12} = K_{21} = 1$ and $K_{22} = 0 \text{ m/sN}$ always satisfies the second and third conditions of Eq. (43) when required and these are fixed parameters in the above three cases. With $b_1 = 1 \text{ Ns/m}$, the varying choice of the parameter K_{11} will be $K_{11} = 1.1 \text{ Ns/m}$ for the active case, $K_{11} = 1 \text{ Ns/m}$ for the limit of passivity and $K_{11} = 0.9 \text{ Ns/m}$ for the dissipative case. In each case, three graphs are displayed as shown in Fig. 20:

- the total energy generated by the internal modulated sources (MSe and MSf),
- the total energy dissipated by the R element,
- and the total energy stored in the system (i.e. by I and C elements).

Fig. 20 (a) shows the simulation results when the system is nonpassive ($K_{11} > b_1$) and the first condition in Eq. (43) is not satisfied. In this case, the stored energy in the system increases over time from its initial value of $E_o = 1.5 \text{ J}$. Graphs of the internally generated energy and the dissipated energy show that the former is greater than the latter and the difference between the two graphs increases with time leading to the system being a net generator of energy and suggesting that an infinite amount of energy could be extracted from the system. In this case, the system is obviously nonpassive and unstable.

Fig. 20 (b) shows the simulation results at the limit of passivity with $K_{11} = b_1 = 1$ Ns/m, $K_{12} = K_{21} = 1$ and $K_{22} = 0$ m/sN. Results show that the energy stored in the system remain constant at its initial value of $E_o = 1.5$ J over time. Both the energy dissipated and the energy generated internally are equal as indicated by their coinciding graphs and, even if both are increasing, the net energy stored in the system is not affected.

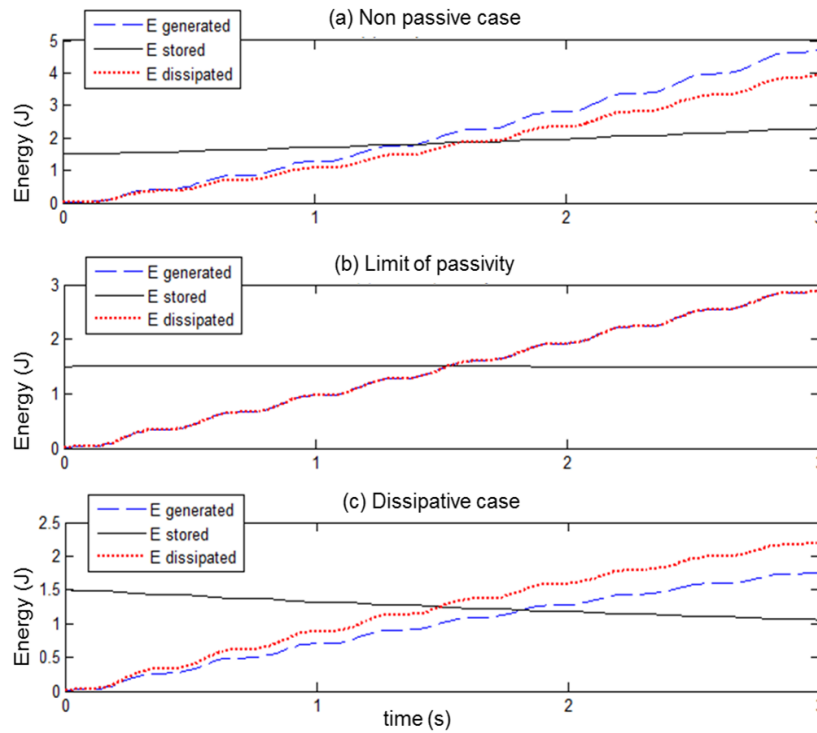


Figure 20. System internal energy for passive and active cases

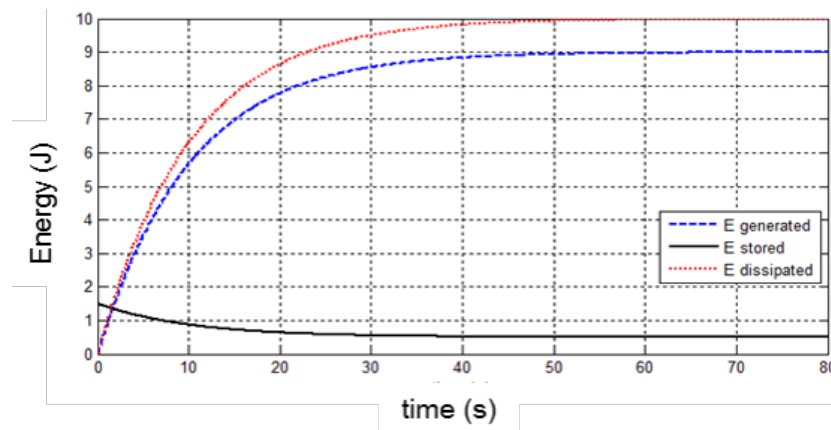


Figure 21. Energy in the steady state of the passive case in Fig. 20(c)

Fig. 20 (c) shows the simulation results when the system is passive ($K_{11} < b_1$). In this case, the energy stored in the system decreases with time from its initial value of $E_o = 1.5$ J. This is also confirmed by the energy dissipated being greater than the energy generated internally with the difference between the two quantities increasing with time until it becomes constant when the system reaches a new steady state at a lower level of internal energy. Fig. 21 shows the same simulation of Fig. 20 (c) for a longer period of time to highlight the steady state of the system at a lower internal energy level of $E = 0.5$

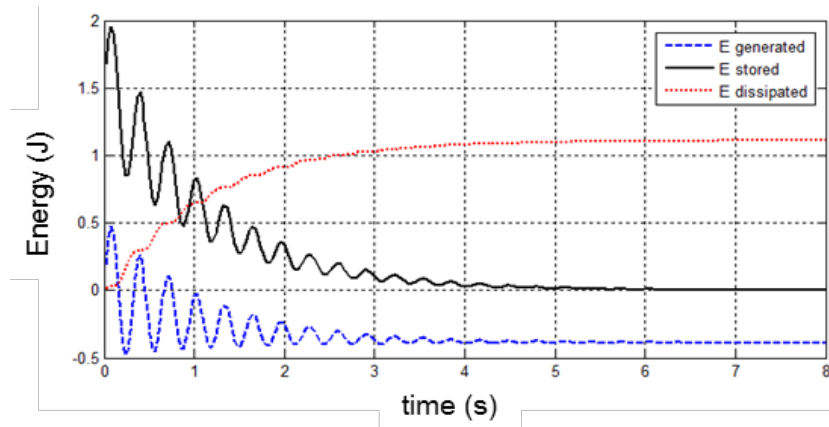


Figure 22. System internal energy for a nonpassive but stable case

J. In this case, the total energy generated by the internal modulated source is 9 J but 10 J are dissipated by the damping element of the system.

In the above simulation results, the case where the system is nonpassive (Fig. 20(a)) suggests that over time, the stored energy in the system will increase indefinitely leading to instability but this is not always the case. Otherwise stated, nonpassivity does not necessarily imply instability even if the converse is true for linear systems. Simulation results in Fig. 22 illustrates this point. Modulating gains used for this simulation are $K_{11} = 0.1$ Ns/m, $K_{12} = 1$, $K_{21} = 0$ and $K_{22} = 0$ m/sN so that the first and third passivity conditions of Eq. (43) are satisfied but the second condition is not, making the closed loop system nonpassive. However, as shown by the simulation in Fig. 22, the system is stable as it eventually settles down to zero in the steady state when all the internal energy is dissipated partly by the R-element (approximately 1.1 J) and partly by the internal sources (around 0.4 J). In this case, the nonpassive behaviour of the system is manifested when its stored energy initially increases over the maximum available $E_o = 1.5$ J set by the initial conditions. Graphs of internal energy generated and energy dissipated also confirm this result with a delay in the dissipative phenomenon during the first 0.15 second.

Simulations results presented in this section illustrate and validate the passivity analysis approach developed in this paper. Potential future work could be concerned with the link between nonpassivity and stability as mentioned in the preceding paragraph. For example, a number of simulations conducted for this simple example show that the first passivity condition $K_{11} \leq b_1$ in Eq. (43) appears to be stronger than the second condition and always leads to nonpassive and unstable system when it is not satisfied. On the other hand, the second condition seems to be weaker and generally leads to nonpassive but stable systems when it is the only condition that is not satisfied.

Conclusions

A general approach to the passivity analysis of linear systems with internal modulated sources modelled by bond graphs is presented in this paper. The approach is based on the proposed *pseudo junction structure* which is an alternative representation of conservative or nonconservative bond graph junction structures in which all the dissipative fields and

internal modulated sources are encompassed into a coupled multiport R-field and separated from an *inner* structure which is conservative (*i.e.* consisting only of TF, GY, 0, 1 junctions). The resulting coupled multiport R-field implicitly performs the balance of internal energy generation and dissipation within the system and the positive semidefiniteness of its constitutive matrix determines the passivity property of the overall system. Two basic configurations namely the cascade interconnection and the closed loop configuration are investigated. Results presented in these two cases can be recursively used for the passivity analysis of complex mechatronic systems. The method also has potential applications in the physical approach to passivity based control design. Future work will look at extending the proposed bond graph based passivity analysis to nonlinear systems.

Acknowledgements

This work was completed when the second author was an academic visitor at the University of Bath and was supported by the CONACyT Sabbatical Project 000000000261575.

References

- [1] A. Achir and C. Sueur. A bond graph procedure for direct passivation of nonlinear systems. In *Proceedings of the European Control Conference*, pages 5729 – 5733, July 2 -55 2007.
- [2] J. J. Beaman and R. C. Rosenberg. Constitutive and modulation structure in bond graph modeling. *Journal of Dynamic Systems, Measurement and Control*, 110:395–402, December 1988.
- [3] W. Borutzky. Bond-graph-based fault detection and isolation for hybrid system models. *Proc. of the Institution of Mechanical Engineers Part I: J. of Systems and Control Engineering*, 226(6):742–760, 2012.
- [4] H. Cormerais, J. Buisson, P. Y. Richard, and C. Morvan. Modelling and passivity based control of switched systems from bond graph formalism: Application to multicellular converters. *Journal of the Franklin Institute*, 345:468 – 488, 2008.
- [5] D. Karnopp, D. L. Margolis, and R. C. Rosenberg. *System Dynamics: A Unified Approach*. John Wiley and Sons, 1975.
- [6] J. D. Lamb, D.R. Woodall, and G. M. Asher. Bond graphs ii: Causality and singularity. *Discrete Applied Mathematics*, 73:143–173, 1997.
- [7] P. Y. Li and R. F. Ngwompo. Power scaling bond graph approach to the passification of mechatronic systems-with application to electrohydraulic valves. *ASME J. of Dynamic Systems, Measurement and Control*, 127(4):633–641, 2005.
- [8] R. Ortega, Z. Liu, and H. Su. Control via interconnection and damping assignment of linear time-invariant systems: a tutorial. *International Journal of Control*, 85(5):603 – 611, 2012.
- [9] J. L. Wyatt, L. O. Chua, J. W. Gannett, I. C. Goknar, and D. N. Green. Energy concepts in the state-space theory of nonlinear n-ports: Part i-passivity. *IEEE Trans. Circ. and Sys*, CAS-28(1):48–61, 1981.

Appendix 1: Effect of scaling matrix in pseudo junction structure of regular bond graph models

With reference to the alternative representation using pseudo junction structures in Figs. 5 and 6, it is shown here that for regular bond graph models (with no internal modulated sources), the effect of multiport scaling matrix reduces to a unit

power scaling factor in the sense that $D_i^T \hat{D}_o = D_i^T D_o$.

From Fig. 5, the multiport scaling matrix is $S_{KD} := -(S_{11}L^{-1} + S_{12})$ and

$$\hat{D}_o = S_{KD}D_o = -(S_{11}L^{-1} + S_{12})D_o \quad (45)$$

Therefore, using Eq. (45), the power at the input port of the power scaling element is

$$D_i^T \hat{D}_o = -D_i^T (S_{11}L^{-1})D_o - D_i^T S_{12}D_o \quad (46)$$

Using the constitutive relationship of the dissipative field $D_o = LD_i$ and knowing that for regular bond graph models, the submatrix S_{11} of the junction structure is skew symmetric due to the continuity of power, the first term at the right hand side of Eq. (46) is null. Also, due to the augmentation of the regular model with parasitic elements, the submatrix $S_{21} = \mathcal{I}$ as stated in Eq. (6) and because of the continuity of power (Property P2), $S_{12} = -\mathcal{I}$. Therefore the second term at the right hand side of Eq. (46) is equal to $D_i^T D_o$. QED \square

Appendix 2: Alternative determination of the matrix of the multiport coupled R-field in Eq. (14) for the model in Fig. 7

The system will be passive if the total power dissipated by the resistances R_1 and R_2 is higher than the power generated by the internal modulated source. Using bonds indexing in Fig. 7, the condition is

$$e_2 f_2 + e_5 f_5 \geq e_4 f_4 \quad (47)$$

Causal relationships and constitutive equations of the resistances and the modulated sources give:

For resistance R_1 :

$$\begin{aligned} e_2 &:= e_3 \\ f_2 &:= e_3/R_1 \end{aligned} \quad (48)$$

For resistance R_2 :

$$\begin{aligned} e_5 &:= e_6 \\ f_5 &:= e_6/R_2 \end{aligned} \quad (49)$$

And for the modulated source MS_F:

$$\begin{aligned} e_4 &:= e_6 \\ f_4 &:= Ke_3 \end{aligned} \quad (50)$$

Combining equations (48), (49) and (50) into equation (47) and rewriting the inequality gives

$$e_3^2/R_1 + e_6^2/R_2 - Ke_3e_6 \geq 0 \quad (51)$$

which is a quadratic inequality that can be written as

$$\begin{bmatrix} \mathbf{e}_3 & \mathbf{e}_6 \end{bmatrix} \begin{bmatrix} 1/R_1 & 0 \\ -K & 1/R_2 \end{bmatrix} \begin{bmatrix} \mathbf{e}_3 \\ \mathbf{e}_6 \end{bmatrix} \geq 0 \quad (52)$$

and is satisfied if the matrix is positive semidefinite. □